Impact of erosion and décollements on large-scale faulting and folding in orogenic wedges: analogue models and case studies

Clement Perrin, Luca Clemenzi, Jacques Malavieille, Giancarlo Molli, Alfredo Taboada, Stéphane Dominguez

Impact of erosion and décollements on large scale faulting and folding in orogenic wedges: analogue models and case studies

Clément Perrin [a, d,*], Luca Clemenzi [a, b, c], Jacques Malavieille [a], Giancarlo Molli [b], Alfredo Taboada [a] and Stéphane Dominguez [a].

[a] Géosciences Montpellier, Université Montpellier 2, Place E. Bataillon, 34095 Montpellier cedex 5, France

[b] Dipartimento di Scienze della Terra, Università di Pisa, Via S.Maria, 53, 56126 Pisa, Italy

[c] Dipartimento di Fisica e Scienze della Terra, Università degli Studi di Parma, Parco Area delle Scienze, 157/A 43100 Parma, Italy

[d] Géoazur, Université de Nice-Sophia Antipolis, Centre National de la Recherche Scientifique (UMR 7329), Observatoire de la Côte d'Azur, 250 av Albert Einstein, 06560 Valbonne, France

* Corresponding author. *Present address*: Géoazur. Université de Nice-Sophia Antipolis, Bât 4, 250 av Albert Einstein, Les Lucioles 1, Sophia-Antipolis 06560 Valbonne, France. Tel.: +33 (0)4 83 61 86 82 / Fax: +33 (0)4 92 94 26 10.

E-mail address: clement.perrin@geoazur.unice.fr (C. Perrin)

5876 words (without references and captions); 114 references; 1 table; 10 figures; 2 figures in supplementary material

Running title : Modeling erosional fold and thrust belts

Abstract: Deformation mechanisms, long-term kinematics and evolution of fold and thrust belts submitted to erosion are studied through 2D analog experiments involving large convergence. First order parameters tested include: i) décollements and/or plastic layers interbedded at different location within analog materials; ii) synconvergence surface erosion.

Weak layers, depending on their location in the model, favor deformation partitioning characterized by the simultaneous development of: i) underplating domains in the inner part of the wedge (basal accretion); ii) frontal accretion where the wedge grows forward. Interaction between tectonics and surface processes influence this behavior. Development of antiformal thrust stacks controlled by underplating show small- and large-scale cyclicity.

Thin plastic layers induce folding processes, which are studied at wedge scale. Recumbent and overturned folds, with large inverted limbs, develop in shear induced asymmetric deformation regime via progressive unrolling of synclinal hinges. Surface erosion and underplating at depth induce further rotation (passive tilting) and horizontalization of fold limbs.

Models results give insights to discuss the mechanisms responsible for the large-scale structures (i.e., antiformal nappe stacks, klippen and kilometer scale recumbent fold-nappes) encountered in several mountain belts such as the Montagne Noire (French Massif Central), the Galicia Variscan belt (Spain) or the Northern Apennines (Italy).

Orogenic wedges are characterized by complex geological structures growing and evolving over long time periods (e.g. Fossen 2010). Their building is mainly controlled by the general mechanics of subduction and by the interactions between tectonics and surface processes that modify wedge dynamics through material transfer (e.g. Malavieille 2010). Because subduction orogens suffer large convergence, the long-term deformation is intense and generates specific structures which mechanisms of genesis are still not completely understood. Among them, the way large-scale recumbent fold-nappes observed in several mountain belt forelands grow and evolve remains enigmatic (Fig. 1). The most beautiful examples in Europe are situated in the Montagne Noire (Southern French Massif Central), Galicia Mountain Belt, (Spain) or the Northern Appennines (Italy). For example, during the Variscan Orogen, large-scale fold-nappes with huge inverted limbs (sometime of more than ten kilometers of amplitude) have been created without (or with very low) metamorphism (e.g. Matte 1968; Arthaud 1970). Other large scale structures are common in mountain belts, such as antiformal stacks of thrust units and subsequent frontal klippen which can be sometimes related to deformation partitioning and subsequent basal accretion of duplex structures (e.g. Elliott & Johnson 1980; Price 1981; Platt *et al.* 1985; Hatcher 1989; Gutscher *et al.* 1996; Burkhard & Sommaruga 1998; Mosar 1999; Kukowski *et al.* 2002; Avouac 2003; Malavieille 2010; Konstantinovskaia & Malavieille 2011; Long *et al.* 2011; Webb *et al.* 2011). Basal accretion activity is generally not constant during the long-term convergent history of orogenic wedges, alternating underthrusting of new tectonic slices with the internal deformation of the already accreted ones, or even with the migration of the underplating locus to a new place. Such a cyclical underplating behavior could promote, at a whole wedge scale, an alternate change from supercritical to subcritical taper condition, in turn favoring

alternations between horizontal and vertical shortening observed in many orogens (e.g. Bell & Johnson, 1989; Bell & Sapkota 2012; Aerden *et al.* 2013). What mechanisms control large scale folding, basal accretion and its cyclicity remain an open question.

Analog modeling is an efficient tool to unravel the main mechanisms controlling the dynamics of orogenic wedges. Various experimental studies have investigated the influence of geometrical, kinematical and rheological parameters on the evolution of thrust wedges (see a review in Graveleau *et al*. 2012). One of the most important parameter highlighted is the layering of the accreting crustal materials that induces mechanical heterogeneity and deformation partitioning. Such a heterogeneous rheology of accreted rock sequences is the result of various factors: stratigraphy of the incoming crustal layer (e.g. Davis & Engelder 1985; Mulugeta 1988; Liu & Dixon 1990; Liu *et al.* 1992; Baby *et al.* 1995; Mandal *et al.* 1997; Nieuwland *et al.* 2000; Costa & Vendeville 2002; Koyi & Vendeville 2003; Konstantinovskaia & Malavieille 2005; Stockmal *et al.* 2007; Malavieille 2010; Smit *et al.* 2010), décollements in a sedimentary sequence or basement-cover interface (e.g. Konstantinovskaia & Malavieille 2011), rheological evolution of the crust due to P-T changes through time (Carry *et al.* 2009; Gueydan *et al.* 2009), or structures and fabrics inherited from an earlier tectonic history (Sutton & Watson 1986; Holdsworth *et al.* 1997; Butler *et al.* 2006, 2008; Bonnet *et al.* 2007, 2008). Among the large number of previous experimental studies of thrust wedges involving multiple décollements, only a few have suggested that faults development and evolution of structures could be cyclical under specific deformation conditions (e.g. Mulugeta & Koyi 1992; Gutscher *et al.* 1998a; Malavieille 2010).

Analog models allow to investigate the importance of surface processes (i.e. erosion and sedimentation) and their influence on the dynamics of accretionary wedges (e.g. Baby *et al.* 1995; Larroque *et al.* 1995; Storti & McClay 1995; Mugnier *et al.* 1997; McClay *et al.* 1999; Persson & Sokoutis 2002; McClay *et al.* 2004; McClay & Whitehouse 2004; Konstantinovskaia & Malavieille 2005, 2011; Graveleau & Dominguez 2008; Cruz *et al.* 2008, 2010; Malavieille 2010; Smit *et al.* 2010). Folding represents another aspect of deformation processes investigated using analog experiments but, although studied at different scales through different experimental setups (e.g. Abbassi & Mancktelow 1990; Grujic & Mancktelow 1995; Tikof & Peterson 1998; Bazalgette & Petit 2007; Noble & Dixon 2011), fold development have rarely been investigated at the scale of a whole accretionary wedge.

This study address five major questions: 1) how do décollements influence deformation partitioning within thrust wedges, and their long term evolution, 2) which mechanisms govern the development of large scale overturned folds commonly preserved in mountain belt forelands as synformal fold-nappes klippen, 3) what controls the growth of large scale antiformal structures that develop concomitantly in the hinterland, 4) what are the interactions between relatively strong plastic layers versus weak décollements, and 5) what is the impact of surface processes on all these mechanisms? We present results of an analog modeling approach that takes into account large amounts of shortening of mechanically heterogeneous, multilayered materials and simultaneous surface erosion. Our first goal is to analyze the role of strain partitioning in relation with material transfer by erosion. Then, we study the impact of thin plastic layers interlayered in the incoming material on folding mechanisms and on its evolution at the scale of a fold and thrust wedge. The main

127 experimental results are discussed and compared to large-scale tectonic structures
128 from several mountain belts to better interpret their geometry and kinematic
129 evolution.
130
131 **Experimental set up and procedure**
132 The experimental set-up simulates the basic geometry and the main mechanisms of a
133 subduction zone where lower plate crustal materials sink beneath an upper plate. This
134 domain of the upper-plate located above the subduction interface corresponds in the
135 experiments to a deformable proto-forewedge equivalent to the units of the orogen
136 already accreted, deformed and structured following subduction. All experiments are
137 performed under normal gravity field in a classical sandbox (see Malavieille 1984 and
138 Konstantinovskaia & Malavieille 2005, 2011), adapted to allow large shortening (over
139 200 cm) and presenting a flexure of the basal plate taking into account the curvature
140 of a subducting plate.
141 The sandbox (Fig. 2) is 10 cm wide and 300 cm long, with a vertical rigid buttress. At
142 the base a thin plastic strip (dacron cloth) exits from the device through a thin slot
143 located at the base of the buttress. It is pulled by a computer controlled step by step
144 electric motor. Analog materials materializing the upper crust rocks of the lower plate
145 are deposited onto the plastic strip and are dragged toward the backstop. As they
146 cannot exit from the device, they are accreted against the upper-plate backstop. A thin
147 layer of sand is glued on the upper surface of the plastic strip, leading to a very rough
148 surface. It creates a high basal friction ($\mu_b \approx 0.5$) between the basal strip and the
149 analogue material of the models. According to the critical wedge theory (Davis *et al.*
150 1983; Dahlen *et al.* 1984; Dahlen 1984), the strength of the basal décollement

151 influences the dipping of the main thrusts and backthrusts and the surface slope angle
152 of a wedge that satisfies the yield conditions.
153
154 Three different materials are used in the models. 1) Aeolian sand, with a density of
155 1690 kg/m3, well rounded grains, less than 300μm in size, coefficient of internal
156 friction (μ_0) is 0.57 and the cohesion (C) is 100-150 Pa. It composes the upper plate
157 protowedge and a large part of lower plate layers. 2) Glass microbeads poured in the
158 sandcake are used to model weak layers (décollements). Diameter is 100/200 μm, and
159 the perfect roundness of the grains leads a smaller coefficient of internal friction (μ_0 =
160 0.44) and a negligible cohesion. 3) Plasticine is used to simulate folding because it
161 presents a plastic behavior. It is composed by mineral oils, waxes and a solid filler
162 made of fine powder (15μm). It does not contain water, does not dry, and can be
163 reused. The Plasticine is melted in an oven (softening point between 39 and 42°C) and
164 poured in a 200 x 9.8 cm mold. After cooling, 1 mm thin layers are sliced and then
165 included in the multilayered model. To observe the final deformation of the plastic
166 layer at the end of experiment, we have carefully cleaned the sand around the fold
167 limbs. Practically, in the experimental procedure, when a plasticine layer is emplaced
168 in the sand cake, the width of the thin plasticine sheet is slightly lower than the space
169 between the two glass sidewalls to avoid parasitic effects of lateral friction along the
170 glass. So, less than 1 mm of sand separates the plastic layer from the sidewall. As a
171 consequence, what we can observe directly through the glass sidewall is not the
172 plasticine layer itself, but the thin coloured sand marker which outlines its
173 deformation.
174
175

176 Aeolian sand and glass microbeads are commonly used in physical modeling studies
177 as analogue of upper crustal rocks with a brittle behavior. The scaling factor between
178 their mechanical properties and those of the natural prototype is 10^5 (Krantz 1991;
179 Schellart 2000; Lohrman *et al.* 2003). The same 10^5 scaling factor is therefore used
180 for model dimensions (1 cm = 1 km), in order to satisfy the fundamental scaling
181 theory for analogue modelling (Hubbert 1937, 1951; Horsfield 1977; Ramberg 1981;
182 Davy & Cobbold 1991; Graveleau *et al*. 2011). Plasticine is a non-Newtonian fluid
183 characterized by strain rate-dependant plastic yielding and strain hardening. At
184 constant temperature, the constitutive flow law for plasticine is given by $\dot{E} = C\sigma^n$,
185 where $\dot{E}$ is the strain rate, C is a material constant, n is a stress exponent, and σ is the
186 differential stress (McClay 1976; Ranalli 1995). The apparent dynamic viscosity (η)
187 of plasticine is given by one half the ratio between the differential stress and the strain
188 rate: $\eta = \sigma/(2\dot{E})$.
189 Considering that experiments were carried at constant room temperature (T ~ 22-
190 25°C) and that the strain rate of the plasticine layer during deformation is constant
191 and very low ($\dot{E} \approx 1 \times 10^{-3}$ s^{-1}) then $\eta \approx 4 \times 10^7$ Pa s. This value of viscosity was
192 determined by mechanical experiments on plasticines (Schöpfer & Zulauf 2002;
193 Zulauf & Zulauf 2004) whose composition is similar to the plasticine used in our
194 analogue models.
195 The yield strength of a plasticine layer with millimetric thickness is roughly
196 equivalent to the compressional strength of a sand layer with centimetric thickness.
197 Thus, the strength contrast between plasticine layers and granular layers (sand or glass
198 microbeads) in our models is roughly equivalent to the strength contrast between
199 ductile yet strong rock layers (such as limestone) and weak rock layers (such as

200 siltstones or shale). This strength contrast is typical of sedimentary sequences
201 observed in foreland and intra-mountainous basins in orogenic wedges.
202
203 Thirteen experiments have been run (Table 1). Among them, seven are chosen as
204 representative to describe the main results of our study. Erosion has been applied to
205 most of them, following the procedure described here below. First, an initial
206 shortening without erosion is applied to the models, allowing the development of a
207 wedge shaped topographic relief. This first step of wedge growth could be considered
208 as the analogue of wedge development in a poorly erosional submarine setting. Then,
209 erosion is applied step by step, each 2 cm of convergence (see digital screen in
210 experiment pictures for shortening values), simulating a climate-dependent erosion in
211 a subaerial wedge setting and keeping a constant evolution of the wedge topography.
212 It is performed by scraping off all the material rising above an imposed erosion
213 surface and then removing it with a vacuum cleaner. The slope of this erosion surface
214 can be variable or fixed and predetermined. In the former case the slope of the erosion
215 surface is adjusted step by step, in order to follow the "instantaneous" average slope
216 of the wedge, just smoothing in this way the small scale irregularities of the
217 topographic profile without altering its average slope. In the latter case an average
218 tilted erosion profile dipping from 3 to 10° toward the foreland is maintained
219 (Konstantinovskaia & Malavieille 2005, 2011; Bonnet *et al.* 2007, 2008). This slope
220 corresponds to the critical taper slope of a dry sand wedge (Davis *et al.* 1983). In this
221 case, local erosion rates are directly controlled by the activity of thrusts. Even if the
222 role of sedimentation has not specifically been taken into account in this study, small
223 piggy back basins that develop during wedge growth have been filled while
224 performing erosion to avoid unrealistic foreland topographies.

Experimental results

Our new set of experiments complements previous modeling works on orogenic processes carried out at the Geosciences Laboratory in Montpellier, which outline the impact of coupling between surface and tectonic processes and the important role of décollement levels during deformation (see, Malavieille *et al*. 1993; Larroque *et al.* 1995; Konstantinovskaia & Malavieille 2005, 2011; Bonnet *et al.* 2007, 2008; Malavieille 2010). Décollement layers favor the mechanical decoupling of stratified material of the subducting plate and consequently, induce deformation partitioning. While upper units are accreted at the toe of the wedge during propagation of the deformation front (frontal accretion), lower units are underthrusted below the main décollement fault and accreted at the base of the wedge by duplexing and underplating (i.e. basal accretion). This partition between vertical and horizontal accretion has a major impact on the organization of tectonic structures, deformation and exhumation of deep units (e.g. Gutscher *et al.* 1998; Bonini 2001, 2003; Adam *et al.* 2002; Kukowski *et al.* 2002; Konstantinovskaia & Malavieille 2005, 2011; Bonnet *et al.* 2007, 2008; Hoth *et al.* 2006, 2007, 2008; Malavieille 2010).

Influence of weak layers

A microbeads layer deposited on the top surface of the lower plate (experiment 1, Fig. 3a) favors underthrusting of the tectonic units below the protowedge in the first steps of experiments. During shortening, the wedge grows mostly in sequence by frontal accretion and shows the typical structure of a simple sand wedge with no décollement in the incoming sequence. We recognize typical structures of high basal friction wedges built up by underthrusting of long tectonic units (e.g. Malavieille *et al.* 1992;

Lallemand *et al.* 1994; Gutscher *et al.* 1998a, 1998b; Nieuwland *et al.* 2000; Agarwal & Agrawal 2002; Kukowski *et al.* 2002; Konstantinovskaia & Malavieille 2005; Graveleau *et al.* 2012). In some cases, when the deformation front advances toward the foreland through the nucleation of a new thrust, the previous frontal thrust remains active until the end of the experiment. Internal deformation of individual foreward vergent thrust units is accommodated by small backthrusts and only few large backthrusts propagate through the whole wedge.

A microbeads layer positioned at ~1/3 of the total lower plate thickness favors remarkable strain partitioning (experiment 4, Fig. 3b). Materials of the upper portion of the subducting plate are deformed by frontal accretion, leading to the development of a typical low basal friction thrust wedge. Given the reduced thickness of the materials deformed by frontal accretion and the reduced basal friction, both the wedge taper angle (Fig. 3b) and the spacing between new thrust faults, are smaller than in experiment 1. Materials of the lower portion of the subducting plate are deformed by underplating and basal accretion (Fig. 3b). As already described in previous papers (e.g. Mulugeta & Koyi 1992; Gutscher 1996, 1998a), underplating is not a steady-state process. More in detail, it can be noted that the evolution of the duplex structure is characterized by the activity of: i) large-offset faults (continuous lines in Fig. 3b and 3c) allowing the accretion of a new unit at the base of the wedge; ii) small-offset faults (dotted lines in Fig. 3b and 3c), allowing the accommodation of the internal deformation of individual underplated units (Adam *et al.* 2002; Kukovski *et al.* 2002; Hoth *et al.* 2008). The large shortening (of the experiments presented in this paper) also allowed a second type of cyclicity to be observed at the whole-wedge scale. When the first antiformal stack of underplated units reaches a critical size, it becomes

inactive and the locus of underplating shifts to a more external position (e.g. toward the foreland) where a second antiformal stack starts developing. The first underplating domain is thus passively accreted and becomes part of the wedge upper-plate. Such a mechanism of accretion repeats itself cyclically during the long-term evolution of a wedge.

Growth of the antiformal stacks leads to some localized uplift of the overlying portion of the wedge as manifested by the shape of the topographic profile, which shows two evident bumps corresponding with the deep duplexes. By contrast the topographic profile is quite regular in wedges lacking strain partitioning (Fig. 3a and 3b).

A microbeads layer located at shallow depth in the sandcake has a slight influence on active deformation, without leading to efficient strain partitioning (experiment 6, Fig. 3d). Only second order small thrust units develop along the weak layer, involving the upper portion of the subducting plate. Such small thrusts are regularly alternated with major thrusts involving the whole subducting plate, and can therefore be considered local splays of the main thrusts. The overall architecture of the wedge is that of a classical high basal friction wedge, similar to the one obtained without microbeads layer (Fig. 3d).

Influence of a plastic layer on folding

In experiment 10 (Fig. 4a) the introduction of a plastic layer in the subducting plate drastically changes the tectonic style and kinematic evolution of the wedge, and leads to folding processes at the scale of a whole accretionary wedge. The main mechanisms of folds development in the experiment with no erosion are described Fig. 5. Development of folds begins by buckling of the plastic layer, which is

accommodated by a pop up structure in the overlying “brittle” sand layer. The wavelength of buckling and the folding mechanism are controlled by the strength contrast between the relatively strong yet ductile plasticine layer and weaker sand layers (see previous section). Soon afterwards, the folding amplitude increases, folds become asymmetric and overturned, controlled by progressive shearing deformation induced by the growth of the prism. Shearing is partly responsible for the development of the long inverted limbs, but the plastic layer is never disrupted or stretched enough to be cut, thus allowing unrolling of the synclinal hinge. Fold growth proceeds by continuous unrolling of the synclinal hinge which causes existing nearby thrusts to become inactive, while new ones form. Then, the inactive faults are passively transported along the inverted fold limb, although some can be reactivated by out-of-sequence thrusting.

Impact of surface erosion

The effect of surface erosion is tested on wedges characterized by different tectonic styles. In experiment 6, a simple high friction thrust wedge showing no strain partitioning or folding is submitted to erosion. It is comparable to experiment 1, except the latter did not include erosion. Figure 3d outlines the similar tectonic styles of both models, and similar taper angle of their pro-wedges.

Experiment 5 (Fig. 3c) shows the effects of erosion on a wedge characterized by strong strain partitioning, to be compared with experiment 4, which has the same initial setup but no erosion. In both models permanent underplating leads to the development of a large antiformal stack formed by basal accretion of duplex units. It induces uprising of internal domain and subsequent localized surface uplift. In model

5, however, surface uplift enhances localized surface erosion, which in return favors further uplift and localization of underplating. As shown in figure 3c the final product of this process is the exhumation of underplated units in localized areas.

In experiment 11 (Fig. 4b) a model involving a plastic layer is submitted to erosion in order to investigate the impact of surface processes on the dynamics of folding. Compared to experiment 10, which has the same initial setup, experiment 11 shows several differences in the general tectonic style. Despite erosion of anticlinal fold hinges, shear deformation increases the length of the inverted sequence, which is associated with the unrolling, and migration of the synclinal fold hinge. Frontal accretion spreads but the amount of shortening accommodated through each folded tectonic unit is higher. The material removed by erosion delays the growth of the wedge and thus its ability to propagate the deformation forward through new tectonic units. Although the anticline hinge is being removed by erosion, unrolling of the syncline hinge continues suggesting that the inverted limb is not submitted to traction. The diffuse shear deformation involved in the core of folds due to asymmetric shortening could be responsible for the forward migration (relative to the undeformed foreland) of the synclinal hinge.

To summarize the main differences, we note that each unit is more intensely deformed and that the length of fold limbs is greater in the experiment with erosion. In addition, for an equivalent amount of shortening, less tectonic units were formed.

Brittle/ductile multilayer and underplating

In experiments 10 and 11, large-scale isoclinals folds developed with an average final overturning of the limbs ranging between 30° and 50°. These modeling results cannot

350 explain what is commonly observed in many natural mountain forelands where large
351 scale inverted fold limbs rest close to horizontal over kilometers. Thus, important
352 questions remain: what mechanism is responsible for the huge overturning observed?
353 And, does this mechanism occur during folds development or by rigid rotation due to
354 late tilting? In order to answer these questions, we have taken into account the
355 insights from the experiments involving basal accretion. As previously shown,
356 décollement layers play a key role during deformation and interactions with surface
357 processes, that seems major too for the development of folding during the growth of
358 fold and thrust belts.
359 In experiment 13 (Fig. 4c) we tested the impact of heterogeneous layering involving
360 décollements, brittle and plastic behaviors (very common in foreland belts). The
361 model combines strain partitioning, folding and surface erosion. A 5 mm thick layer
362 of sand is placed between a 1 mm thick plasticine sheet and the 3 mm thick weak
363 layer of glass microbeads. The complete evolution of the experiment is described in
364 the figure 6. Erosion begins after 15 cm of shortening and the wedge slope is
365 sustained at about 3° during shortening (60% at the end of the experiment). During
366 convergence, fold hinges are rapidly eroded, while active thrusting occurs in the core
367 of folds. Six folded tectonic units were obtained and a large domain of deeply
368 accreted units is exhumed behind the prism. Note that we also observed the cyclical
369 behavior of underplating as described previously.
370 The structures located above the décollement layer are passively deformed and
371 uplifted due to basal accretion, tilting the back part of folded tectonic units. These
372 deep accretionary processes are responsible for the important overturning and rotation
373 of the flanks of folded structures. During continuous shortening, the kinematics of
374 deformation reflects the complex interaction between wedge mechanics and erosion.

At the final stage most of the folded units from the backpart of the wedge have been removed by erosion. Finally, three different tectonic domains characterized by specific deformation features are juxtaposed. From the frontal part of the wedge to the backstop respectively, we have (Fig. 6): a frontal imbricate of thrust and fold sheets; a synformal klippe of folded units previously accreted to the front and progressively deformed; and, an antiformal stack of underplated thrust units refolding the upper décollement layer.

Discussion and case studies

Results of this series of experiments give some insights for the interpretation of several debated features of the forewedge domain of mountain belts formed in continental subduction settings. Chosen case studies are discussed in the light of our experimental results. The last model, which contains the main features described in previous sections, is used to illustrate the general mechanisms explaining the relationships between the main tectonic units of natural orogenic wedges (Fig. 7).

Examples from the Variscan Belt

The Variscan orogen developed during the Gondwana-Laurasia collision from Devonian to middle Carboniferous times (e.g. Matte 2007). The Montagne Noire in southern French Massif Central and the Galicia Mountains in northwest Spain represent segments of this orogen characterized by a foreland fold and thrust belt domain associated with a syntectonic foreland basin (e.g. Arthaud 1970; Matte 1968; Pérez-Estàun *et al.* 1991; Simancas *et al*. in press). Low-grade tectonic units mainly composed by sedimentary rocks of the Paleozoic cover (schists, limestones and quartzites of Cambrian to Carboniferous ages) are intensely folded and juxtaposed

400 with antiformal stacks of Proterozoic to Cambrian metamorphic basement rock units
401 largely exhumed in the hinterland. The Montagne Noire which forms the
402 southernmost part of the Variscan French Massif Central (Fig. 8) is generally
403 subdivided into three tectonostratigraphic units (e.g. Gèze 1949; Arthaud 1970). (1) A
404 Northern Flank upper-plate unit with a southward tectonic vergence, consists of
405 folded and faulted low-grade lower Paleozoic metasedimentary rocks. (2) An Axial
406 Zone lower-plate unit, is formed by an antiformal structure of crystalline rocks
407 (gneiss, migmatite, and micaschist) of Proterozoic to Ordovician age. This
408 metamorphic domain composed by high grade rocks has been variously interpreted in
409 terms of : diapirism (e.g. Gèze 1949; Beaud 1985 ; Charles *et al.* 2009), contractional
410 tectonics (Arthaud *et al.* 1966; Mattauer *et al*. 1996; Aerden & Malavieille, 1999;
411 Soula *et al.* 2001; Matte, 2007; Malavieille 2010), emplacement in a crustal scale
412 strike-slip setting (e.g. Nicolas *et al.* 1977; Franke *et al.* 2011), or as extensional
413 metamorphic core complex (e.g. Echtler & Malavieille, 1990; Van den Driessche &
414 Brun 1992). In fact, most authors agree on the geological evidences for a
415 contractional history followed (or assisted) by gravity induced extensional processes
416 favoring exhumation, detachment formation and diapirism in the evolutionary stages
417 of the orogen. (3) A Southern Flank, well known in the literature for the kilometer-
418 scale recumbent fold nappes, is composed by very low-grade Paleozoic sedimentary
419 sequences. The south verging nappes stack is intimately associated with syntectonic
420 Visean flysch sediments deposited in a foreland basin setting, in a shallow marine
421 environment. The upper-plate nappes are separated from high-grade lower-plate
422 basement units by major fault zones that record a complex pattern of deformation
423 (e.g. Echtler & Malavieille 1990; Aerden & Malavieille 1999). Figure 8 shows an
424 interpreted cross section of The Montagne Noire (Malavieille 2010).

Similar key structures of the Galicia Mountain Belt are outlined on the cross-section of figure 9, modified from Pérez-Estàun *et al*. (1991). Proterozoic metamorphic units outcrop in the internal domain while a domain of large scale recumbent folds made of Cambrian quartzite/limestone characterizes external foreland units. These kilometric scale folds present horizontal or overtilted limbs (Matte 1968; Pérez-Estàun *et al.* 1991). Note that in this segment of the Variscan belt, a cyclical basal accretion may have occurred at large scale, as two antiformal stack structures formed during wedge growth.

Comparing wedges architecture and analog models, we can outline geometrical and kinematic similarities. As observed in models involving décollements and brittle/plastic behavior, there is a good analogy between the geometric configuration of the folded superficial domain and the underlying deeper structures. Where underplating develops, the folded units located above the décollement layer are strongly tilted by subsequent uplift in the antiformal stack domain. This can be compared to the fold-nappes structures of the Galicia belt or Montagne Noire. In the parts of the orogenic wedge located far from the locus of basal accretion, large scale folds are simply overturned. During the growth of the Montagne Noire, syntectonic flysches (Visean) are deposited at the toe of the wedge due to erosion of developing fold nappes (Southern flank). At the same time, basal accretion is active during the growth of the prism involving underthrusting of sliced Proterozoic basement and subsequent uplift at the back of the overturned fold domain. Already deformed Upper Paleozoic units are overtilted by progressive uplift. The décollement layer allowing strain partitioning between shallow and deep parts of the wedge is located along the

449 main inherited discontinuity, between the crystalline basement and the Paleozoic
450 cover.
451 Figure 6 highlights the major effect of erosion on deformation processes. During
452 wedge growth, due to combined basal accretion, surface uplift and erosion,
453 continuous folding affects tectonic units of the upper-plate that remain at the same
454 structural level in the upper crust whereas large domains of deep metamorphic units
455 of the lower-plate are exhumed. Thus, the deformation mechanisms highlighted in our
456 study may explain how the large scale recumbent fold-nappes with inverted limbs of
457 10 km develop, and why they suffered only slight or no metamorphism.
458
459 *Northern Apennines*
460 The Apennines are a fold and thrust mountain chain constituting the backbone of the
461 Italian peninsula. Figure 10a outlines some aspects of the northernmost portion of this
462 chain (e.g. Molli 2008). The internal zone is characterized by a metamorphic core
463 where two main exhumed tectonostratigraphic units outcrop. The lowermost is the
464 Apuane unit, a low grade metamorphic unit showing greenschist assemblages
465 (deepest estimated burial: ~ 20 km). On the western side of the core, the Apuane unit
466 is overlaid by the Massa unit, an HP greenschist facies metamorphic unit with higher
467 grade P/T peak conditions (estimated deepest burial: ~ 25/30 km). The whole
468 metamorphic core is overlaid by the Tuscan Nappe, an anchimetamorphic unit with a
469 deepest estimated burial of ~ 7 km, which in turn is overlaid by Subligurian and
470 Ligurian non-metamorphic units and by the Epiligurian basin (e.g. Fellin *et al.* 2007
471 and references therein). In a central portion, east of the Alpi Apuane, the chain is
472 characterized by a recumbent fold domain (Fig. 10b) where the Tuscan Nappe is
473 folded in a kilometric-scale recumbent structure (the Val di Lima fold), with an

outcropping kilometers long inverted limb. This recumbent fold shows minor structures related with superimposed deformations (Baldacci *et al.* 1992; Fazzuoli *et al.* 1998) with development of the long inverted limb by progressive hinge migration (Botti *et al*. 2010).

The overall geometrical configuration of the analyzed segment of the Apennines (Fig. 10) can be interpreted in the light of our models. The combined action of basal accretion and underplating of tectonic units produced the growth of a syn-metamorphic antiformal stack (Molli & Vaselli 2006) responsible of strong uplift and exhumation by submarine (in the early stages) and later surface erosion (Molli *et al.* 2002; Fellin *et al.* 2007). Erosion-processes were associated with tectonic thinning by normal-slip reactivation of the basal thrust of the unmetamorphic units at the hanging wall and the metamorphic core at the footwall (Carmignani & Kligfield 1990; Molli *et al.* 2002; Fellin *et al.* 2007; Molli 2008). Moreover, the growth of the antiformal stack may have induced progressive tilting of the basal detachment and the formation of recumbent geometry of the folded Tuscan unit in the Lima Valley (Fig.10a,b).

Indeed, the locus of basal accretion and the folded domain are close enough to presume the influence of the underlying deep structures on the passive rotation of the fold limbs. Model results can give some more hints on the processes that may have influenced the geological evolution of the metamorphic core, suggesting that two successive episodes of underplating, could have been responsible for the syn-contractional juxtaposition of the Massa unit above the Apuan unit.

Open questions in other mountain belts

Mechanisms responsible for deformation structures and exhumation processes developed in the Himalayas are presently widely discussed through two main kind of

499 models (ductile channel flow, e.g. Nelson *et al.* 1996; Beaumont *et al*. 2001; Jamieson
500 *et al.* 2004; and wedge extrusion in a thrust system, e.g. Burchfiel & Royden 1985;
501 England & Molnar 1993; Guillot & Allemand 2002, Webb *et al.* 2007, Kali *et al.*
502 2010). Our study outline simple mechanisms that seem to be consistent with the
503 observed large-scale geological structures (antiformal stacks, synformal klippen of
504 fold and thrust units), in agreement with the second orogenic wedge model.
505
506 **Conclusions**
507 Interaction between climate controlled surface processes including erosion,
508 sedimentation and deformation processes plays a key role in the structural evolution,
509 kinematics and exhumation of rocks in orogenic wedges. During continental
510 subduction, the role of the rheologic layering of the crust can be major as it
511 determines the partitioning of deformation in a growing orogenic wedge into domains
512 undergoing horizontal and vertical accretion. Partitioning is first controlled by
513 tectonic processes, but material transfer induced by surface processes exerts a strong
514 feed-back on wedge dynamics. Insights from analog models applied to natural cases
515 allow us to emphasize several first order interaction mechanisms that result from this
516 coupling. Experiments show that strain partitioning is not systematic but depends on
517 the position of weak layers in the layered incoming sequence. They show a cyclical
518 behavior of basal accretion, leading to episodic underplating of tectonic units, which
519 has a strong impact on the vertical component of displacement of rock material. In
520 turn, it changes surface slopes favoring erosion in domains of strong surface uplift. In
521 addition, our experiments offer an explanation for the enigmatic domains of non
522 metamorphic large scale fold nappes units observed in the foreland of many orogenic
523 wedges. To a first order, the dynamics of folding involves rolling of a synclinal hinge

524 and develop exclusively overturned fold types. This mechanism was observed, in
525 particular, for multilayered models constituted of both strong yet ductile layers and
526 comparatively weaker granular layers.
527 The influence of the deep wedge dynamics, such as the growth of basal duplexes,
528 causes further rotation of fold structures, leading to the horizontalization of fold
529 limbs, while erosion processes keep the folded units in a superficial low-grade
530 metamorphic domain. Natural wedges (e.g. Galicia, Montagne Noire and Northern
531 Apennines) present close similarities to the experiments described herein, both in
532 terms of architecture and orogenic dynamics. Other orogenic wedges exposing similar
533 structures such as exhumed antiformal metamorphic domes juxtaposed with domains
534 of largely folded upper-crustal rock sequences need to be revisited in the light of the
535 general mechanisms here outlined.
536 Future work should concentrate on multilayered models with different rheological
537 contrasts (e.g. weak ductile layers and strong brittle layers) to determine other
538 possible large-scale folding mechanisms in the shallow domains of orogenic wedges.
539
540
541 **Acknowledgements**
542 Our modeling work has benefitted from the technical assistance of C. Romano. Many
543 thanks to Nina Kukowski who helped us improving an early version of the
544 manuscript. This study has been partly funded in the frame of the ACTS ANR project.
545 The contibution by Clemenzi has benefitted from an Erasmus Placement exchange
546 and funding between Pisa and Montpellier Universities. This paper benefitted from
547 constructive review by D.G.A.M. Aerden and an anonymous reviewer.
548

549

550 **References**

551 ABBASSI, M. R. & MANCKTELOW, N. S. 1990. The effect of initial perturbation shape
552 and symmetry on fold development. *Journal of Structural Geology*, **12**, 273–282.

553

554 ADAM, J., LOHRMANN, J., HOTH, S., KUKOWSKI, N. & ONCKEN, O. 2002. Strain
555 variation and partitioning in thrust wedges: high-resolution data from scaled sandbox
556 experiments by 2D–3D PIV analysis. *Bollettino di Geofisica Teorica ed Applicata*,
557 **42**, 123–125.

558

559 AERDEN, D. G. A. M. & MALAVIEILLE, J. 1999. Origin of a large-scale fold nappe in
560 the Montagne Noire, Variscan belt, France. *Journal of Structural Geology*, **21**, 1321–
561 1333.

562

563 AERDEN, D. G. A. M., BELL, T. H., PUGA, E., SAYAB, M., LOZANO, J. A. & DIAZ DE
564 FEDERICO, A. 2013. Multi-stage mountain building vs. relative plate motions in the
565 Betic Cordillera deduced from integrated microstructural and petrological analysis of
566 porphyroblast inclusion trails. *Tectonophysics,* **587**, 188–206

567

568 AGARWAL, K. K. & AGRAWAL, G. K. 2002. Analogue sandbox models of thrust
569 wedges with variable basal frictions. *Gondwana Research*, **5**, 641-647.

570

571 ARTHAUD, F. 1970. Etude tectonique et microtectonique comparée de deux domaines
572 Hercyniens : les nappes de la Montage Noire (France) et l'anticlinorum de l'Iglesiente
573 (Sardaigne). *Publications de l'université des Sciences et Techniques du Languedoc,*

574 *Montpellier.* Série Géologie Structurale, **1**.
575
576 ARTHAUD, F., MATTAUER, M. & PROUST, F, 1966. La structure et la microtectonique
577 des nappes hercyniennes de la Montagne Noire. Colloque "Étages Tectoniques",
578 Neuchâtel, 231–247.
579
580 AVOUAC, J. P. 2003. Mountain Building, Erosion, and the Seismic Cycle in the Nepal
581 Himalaya. *In: Advances in Geophysics*, Elsevier, **46**, 1-80.
582
583 BABY, P., COLLETTA, B. & ZUBIETA, D. 1995. Etude géométrique et expérimentale
584 d'un bassin transporté: exemple du synclinorium de l'Alto Beni (Andes centrales).
585 *Bulletin de la Société Géologique de France*, **166**, 797-811.
586
587 BALDACCI, F., CARMIGNANI, L., FANTOZZI, P., MECCHERI, M. & PLESI, G. 1992.
588 Lineamenti stratigrafico-strutturali lungo la trasversale Alpi Apuane - Appennino
589 reggiano-modenese. *Studi Geol. Camerti*, Vol. Spec., 31-49.
590
591 BAZALGETTE, L. & PETIT, J. P. 2007. Fold amplification and style transition involving
592 fractured dip-domain boundaries: buckling experiments in brittle paraffin wax
593 multilayers and comparison with natural examples. *In:* LONERGAN, L., JOLLY, R.J.H.,
594 RAWNSLEY, K. & SANDERSON, D. J. (eds) *Fractured Reservoirs*. Geological Society,
595 London, Special Publications, **270**, 157–169.
596
597 BEAUD, F. 1985. Etude structurale de la Zone Axiale orientale de la Montagne Noire
598 (Sud du Massif Central Français). Détermination des mécanismes de déformation.

599 Relation avec les nappes du Versant Sud. Thèse 3ème cycle, Université des Sciences
600 et Techniques du Languedoc, Montpellier, 191 p.
601
602 BEAUMONT, C., JAMIESON, R. A., NGUYEN M. H. & LEE, B. 2001. Himalayan tectonics
603 explained by extrusion of a low-viscosity crustal channel coupled to focused surface
604 denudation, *Nature*, **414**, 738–742, doi:10.1038/414738a
605
606 BELL, T. H. & JOHNSON, S. E. 1989. Porphyroblast inclusion trails: the key to
607 orogenesis. *Journal of Metamorphic Geology*. **7**, 279–310, doi:10.1111/j.1525-
608 1314.1989.tb00598.x
609
610 BELL, T. H. & SAPKOTA, J. 2012. Episodic gravitational collapse and migration of the
611 mountain chain during orogenic roll-on in the Himalayas. *Journal of Metamorphic*
612 *Geology*, **30**, 651–666, doi: 10.1111/j.1525-1314.2012.00992.x
613
614 BONINI, M. 2001. Passive roof thrusting and forelandward fold propagation in scaled
615 brittleductile physical models of thrust wedges. *Journal of Geophysical Research*,
616 **106**(B2), 2291-2311.
617
618 BONINI, M. 2003. Detachment folding, fold amplification, and diapirism in thrust
619 wedge experiments. *Tectonics*, **22**(6): 1065.
620
621 BONNET, C., MALAVIEILLE, J. & MOSAR, J. 2007. Interactions between tectonics,
622 erosion, and sedimentation during the recent evolution of the Alpine orogen:
623 Analogue modeling insights. *Tectonics*, **26**, TC6016, doi : 10.1029/2006TC002048.

624

625 BONNET, C., MALAVIEILLE, J. & MOSAR, J. 2008. Surface processes versus kinematics
626 of thrust belts: impact on rates of erosion, sedimentation, and exhumation – Insights
627 from analogue models. *Bulletin de la Société Géologique de France*, **179**, 179-192.

628

629 BOTTI, F., DANIELE, G., BALDACCI, F. & MOLLI, G. 2010. Note Illustrative della Carta
630 Geologica d'Italia alla scala 1: 50.000, Foglio 251 Porretta Terme. *Servizio Geologico*
631 *d'Italia, Regione Emilia-Romagna*.

632

633 BURCHFIEL, B. C. & ROYDEN, L. H., 1985. North-south extension within the
634 convergent Himalayan region, *Geology*, **13**, 679–682

635

636 BURKHARD, M. & SOMMARUGA, A. 1998. Evolution of the western Swiss Molasse
637 basin: structural relations with the Alps and the Jura belt. *In:* MASCLE, A,
638 PUIGDEFABREGAS, C., LUTERBACHER, H.P. & FERNANDEZ, M. (eds) *Cenozoic*
639 *Foreland Basins of Western Europe*. Geological Society, London, Special
640 Publications, **134**, 279-298.

641

642 BUTLER, R. W. H., TAVARNELLI, E. & GRASSO, M. 2006. Structural inheritance in
643 mountain belts : An Alpine-Apennine perspective. *Journal of Structural Geology*, **28**,
644 1893–1908.

645

646 BUTLER, R. W. H., BOND, C. E., SHIPTON, Z. K., JONES, R. R. & CASEY, M. 2008.
647 Fabric anisotropy controls faulting in the continental crust. *Journal of the Geological*
648 *Society, London*, **165**, pp. 449–452.

649

650 CARMIGNANI, L. & KLIGFIELD, R. 1990. Crustal extension in the Northern Apennines:
651 the transition from compression to extension in the Alpi Apuane Core Complex.
652 *Tectonics*, **9**, 1275-1303.

653

654 CARRY, N., GUEYDAN, F., BRUN, J. P. & MARQUER, D. 2009. Mechanical decoupling
655 of high-pressure crustal units during continental subduction. *Earth and Planetary*
656 *Science Letters*, **278**, 13–25.

657

658 CHARLES, N., FAURE, M., AND CHEN, Y. 2009. The Montagne Noire migmatitic dome
659 emplacement (French Massif Central): new insights from petrofabric and AMS
660 studies. *Journal of Structural Geology*, **31**, 1423–1440, doi:10.1016/j.jsg.2009.08.007

661

662 COSTA, E. & VENDEVILLE, B. E. 2002. Experimental insights on the geometry and
663 kinematics of fold-and-thrust belts above weak, viscous evaporitic décollement.
664 *Journal of Structural Geology,* **24,** 1729–1739.

665

666 CRUZ, L., TEYSSIER, T., PERG, L., TAKE, A. & FAYON, A. 2008. Deformation,
667 exhumation, and topography of experimental doubly-vergent orogenic wedges
668 subjected to asymmetric erosion. *Journal of Structural Geology*, **30**, 98–115.

669

670 CRUZ, L., MALINSKI, J., WILSON, A., TAKE, W. A. & HILLEY, G. 2010. Erosional
671 control of the kinematics and geometry of fold‐ and‐ thrust belts imaged in a physical
672 and numerical sandbox. *Journal of Geophysical Research*, **115**, B09404,
673 doi:10.1029/2010JB007472.

DAHLEN, F.A. 1984. Non cohesive critical coulomb wedges: an exact solution. *Journal of Geophysical Research*, **89**, 10125-10133.

DAHLEN, F. A., SUPPE, J. & DAVIS, D. 1984. Mechanics of fold-and-thrust belts and accretionary wedges: cohesive coulomb theory. *Journal of Geophysical Research*, **89**, 10087-10101.

DAVIS, D., SUPPE, J. & DAHLEN, F. A. 1983. Mechanics of fold-and-thrust belts and accretionary wedges. *Journal of Geophysical Research*, **88**, 1153-1172.

DAVIS, D. & ENGELDER T. 1985. The role of salt in fold-and-thrust belts. *Tectonophysics*,**119**, 67–88

DAVY, P. & COBBOLD, P. R. 1991. Experiments on shortening of a 4-layer model of the continental lithosphere. *Tectonophysics*, **188**, 1-25.

ECHTLER, H., & MALAVIEILLE, J. 1990. Extensional tectonics, basement uplift and Stephano- Permian collapse basin in a late Variscan metamorphic core complex (Montagne Noire, southern Massif Central). *Tectonophysics*, **177**, 125–138.

ENGLAND, P., & MOLNAR, P. 1993. Cause and effect among thrust and normal faulting, anatectic melting and exhumation in the Himalaya. In: TRELOAR, P. J., SEARLE, M. P. (Eds.), *Himalayan Tectonics*. Geological Society, London, Special Publications, **74**, 401–411.

ELLIOTT, D., & JOHNSON, M. R. W. 1980. Structural evolution in the northern part of the Moine thrust belt, NW Scotland. *Edinburgh Geological Society Transactions, Earth Sciences*, **71**, 69–96.

FAZZUOLI, M., BECARELLI, S., BURCHIETTI, G., FERRINI, G., GARZONIO, C.A., MANNORI, G., SANI, F. & SGUAZZONI, G. 1998. Geologia del nucleo Mesozoico della Val di Lima (Provincie di Pistoia e Lucca, Appennino settentrionale). Note illustrative della carta geologica (Scala 1: 25.000). *Bollettino della Società Geologica Italiana*, **117**, 479-535.

FELLIN, M. G., REINERS, P. W., BRANDON, M. T., WÜTHRICH, E., BALESTRIERI M. L. & MOLLI, G. 2007. Thermochronologic evidence for the exhumational history of the Alpi Apuane metamorphic core complex, northern Apennines, Italy. *Tectonics*, **26**, TC6015, doi:10.1029/2006TC002085

FOSSEN, H. 2010. Structural Geology, *Cambridge University Press*, 463 pp., ISBN-13 978-0-521-51664-8

FRANKE, W., DOUBLIER, M. P., KLAMA, K., POTEL, S. & WEMMER, K. 2011. Hot metamorphic core complex in a cold foreland. *International Journal of Earth Sciences*, **100**, 753-785, doi:10.1007/s00531-010-0512-7.

GÈZE, B. 1949. Etude géologique de la Montagne Noire et des Cévennes méridionales. *Mémoires de la société géologique de France*, **62**, 1–215.

GRAVELEAU, F. & DOMINGUEZ, S. 2008. Analogue modelling of the interaction between tectonics, erosion and sedimentation in foreland thrust belts. *C.R. Géoscience*, **340**, 324–333

GRAVELEAU, F., HURTREZ, J.-E., DOMINGUEZ, S. & MALAVIEILLE, J. 2011. A new experimental material for modeling relief dynamics an interactions between tectonics and surface processes. *Tectonophysics*, **513**, 68-87.

GRAVELEAU, F., MALAVIEILLE, J. & DOMINGUEZ, S. 2012. Experimental modelling of orogenic wedges: A review. *Tectonophysics*, **538**, 1-66.

GRUJIC, D. & MANCKTELOW, N.S. 1995. Folds with axes parallel to the extension direction: an experimental study. *Journal of Structural Geology*, **17**, 279-291

GUEYDAN, F., LE GARZIC, E. & CARRY, N. 2009. P/T ratio in high-pressure rocks as a function of dip and velocity of continental subduction. *Lithosphere*, **1**, 282–290.

GUILLOT, D., & ALLEMAND, P. 2002. Two dimensional thermal modelling of the early tectonometamorphic evolution in central Himalaya, *Journal of. Geodynamics,* **34**, 77–98, doi:10.1016/S0264-3707(02)00016-9.

GUTSCHER, M. A., KUKOWSKI, N., MALAVIEILLE, J. & LALLEMAND, S. 1996. Cyclical behavior of thrust wedges: Insights from high basal friction sandbox experiments. *Geology*, **24**, 135-138.

GUTSCHER, M. A., KUKOWSKI, N., MALAVIEILLE, J. & LALLEMAND, S. 1998a. Episodic Imbricate thrusting & underthrusting; Analog experiments and Mechanical Analysis applied to the Alaskan Accretionary Wedge. *Journal of Geophysical Research.*, **103**, 10161-10176.

GUTSCHER, M. A., KUKOWSKI, N., MALAVIEILLE, J. & LALLEMAND, S. 1998b. Material transfer in accretionary wedges from analysis of a systematic series of analog experiments. *Journal of Structural Geology*, **20**, 407–416.

HATCHER JR, R. D. 1989. Tectonic synthesis of the U.S. Appalachians. *In:* HATCHER, R.D., THOMAS, W.A., AND VIELE, G.W. (eds), *The Appalachian-Ouachita Orogen in the United States : Boulder, Colorado*. The Geology of North America, **F-2**, 511–535.

HOLDSWORTH, R. E., BUTLER, C. A. & ROBERTS, A. M. 1997. The recognition of reactivation during continental deformation. *Journal of the Geological Society, London,* **154**, 73–78.

HORSFIELD, W. 1977. An experimental approach to basement-controlled faulting. *Geologie en Mijnbouw*, **56**, 363-370.

HOTH, S., ADAM, J., KUKOWSKI, N. & ONCKEN, O. 2006. Influence of erosion on the kinematics of bivergent orgens. Results from scaled sandbox simulations. *In:* WILLETT, S.D., HOVIUS, N., BRANDON, M.T., FISHER, D.M. (eds), *Tectonics, Climate, and Landscape Evolution*. The Geological Society of America, Boulder, Colorado,

774 Special Paper, **398**, 201–225.

775

776 HOTH, S., HOFFMANN-ROTHE, A. & KUKOWSKI, N. 2007. Frontal accretion: an internal
777 clock for bivergent wedge deformation and surface uplift. *Journal of Geophysical*
778 *Research*, **112**, B06408. doi:10.1029/2006JB004357.

779

780 HOTH, S., KUKOWSKI, N. & ONCKEN, O. 2008. Distant effects in bivergent orogenic
781 belts—how retro-wedge erosion triggers resource formation in pro-foreland basins.
782 *Earth and Planetary Science Letters*, **273**(1–2), 28–37.

783

784 HUBBERT, M. K. 1937. Theory of scale models as applied to the study of geologic
785 structures. *Bulletin of the Geological Society of America*, **48**, 1459-1519.

786

787 HUBBERT, M. K. 1951. Mechanical basis for certain familiar geologic structures.
788 *Bulletin of the Geological Society of America*, **62**, 355-372.

789

790 JAMIESON, R. A., BEAUMONT, C., MEDVEDEV, S. & NGUYEN, M. H. 2004. Crustal
791 channel flows: 2. Numerical models with implications for metamorphism in the
792 Himalayan-Tibetan orogen, *Journal of Geophysical Research*, **109**, B06407,
793 doi:10.1029/2003JB002811.

794

795 KALI, K. E., LELOUP, P. H., ARNAUD, N., MAHEO, G., DUNYI LIU, BOUTONNET, E.,
796 VAN DER WOERD, J., XIAOHAN LIU, JING LIU-ZENG, AND HAIBING LI 2010.
797 Exhumation history of the deepest central Himalayan rocks, Ama Drime range: Key
798 pressure-temperature-deformation-time constraints on orogenic models. *Tectonics*,

29, TC2014, doi:10.1029/2009TC002551

KONSTANTINOVSKAIA, E. & MALAVIEILLE, J. 2005. Erosion and exhumation in accretionary orogens: Experimental and geological approaches. *Geochemistry, Geophysics, Geosystems*, **6**, Q02006, doi:10.1029/2004GC000794, ISSN: 1525-2027

KONSTANTINOVSKAIA, E. & MALAVIEILLE, J. 2011. Thrust wedges with décollement levels and syntectonic erosion: A view from analogue models. *Tectonophysics*, 502 336–350, 10.1016/j.tecto.2011.01.020.

KOYI, H. A. & VENDEVILLE, B. C. 2003. The effect of décollement dip on geometry and kinematics of model accretionary wedges. *Journal of Structural Geology,* **25**, 1445-1450.

KRANTZ, R. W. 1991. Measurements of friction coefficients and cohesion for faulting and fault reactivation in laboratory models using sand and sand mixtures. *Tectonophysics*, **188**, 203-207.

KUKOWSKI, N., LALLEMAND, S., MALAVIEILLE, J., GUTSCHER, M.A. & RESTON T.J. 2002. Mechanical decoupling and basal duplex formation observed in sandbox experiments with application to the Western Mediterranean Ridge accretionary complex. *Marine Geology*, **186**, 29–42

LALLEMAND, S., SCHNURLE, P. & MALAVIEILLE, J. 1994. Coulomb theory applied to accretionary and non-accretionary wedges - Possible causes for tectonic erosion

824 and/or frontal accretion. *Journal of Geophysical Research*, **99**(B6), 12033-12055.
825
826 LARROQUE, C., CALASSOU, S., MALAVIEILLE, J. & CHANIER, F. 1995. Experimental
827 modelling of forearc basin development during accretionary wedge growth. *Basin*
828 *Research*, **7**(3), 255–268.
829
830 LIU, S. & DIXON, M. 1990. Centrifuge modelling of thrust faulting: strain partitioning
831 and sequence of thrusting in duplex structures. *Geological Society, London, Special*
832 *Publications.* **54***,* 431-444.
833
834 LIU, H., MCCLAY, K. & POWELL, D. 1992. Physical models of thrust wedges. *In:*
835 MCCLAY K. (ed) *Thrust Tectonics*. Chapman and Hall, London, 71-81.
836
837 LOHRMAN, J., KUKOWSKI, N., ADAM, J. & ONCKEN, O. 2003. The impact of analogue
838 material properties on the geometry, kinematics, and dynamics of convergent sand
839 wedges. *Journal of Structural Geology*, **25**, 1691–1711.
840
841 LONG, S., MCQUARRIE, N., TOBGAY, T. & HAWTHORNE, J. 2011. Quantifying internal
842 strain and deformation temperature in the eastern Himalaya, Bhutan: Implications for
843 the evolution of strain in thrust sheets. *Journal of Structural Geology*, **33**, doi:
844 10.1016/j.jsg.2010.12.011
845
846 MALAVIEILLE, J. 1984. Modélisation expérimentale des chevauchements imbriqués:
847 Application aux chaînes de montagnes. *Bulletin de la Société Géologique de France*,
848 **26**, 129–138.

MALAVIEILLE, J. 2010. Impact of erosion, sedimentation, and structural heritage on the structure and kinematics of orogenic wedges: Analog models and case studies. *GSA Today*, **20**, doi: 10.1130/GSATG48A.1

MALAVIEILLE, J., CALASSOU, S., LALLEMAND, S. & LARROQUE, C. 1992. Experimental modeling of accretionary wedges. Série cours M037, Producted and realized by SNEA(P), France, 28 min.

MALAVIEILLE, J., LARROQUE, C., CALASSOU, S. 1993. Modelisation experimentale des relations tectonique/sedimentation entre bassin avant-arc et prisme d'accretion. *Comptes rendus de l'Académie des sciences*, **316**, 8, 1131-1137

MANDAL, N., CHATTOPHDHYAY, A. & BOSE, S. 1997. Imbricate thrust spacing: experimental and theoritical analyses. *In:* SENGUPTA, S. (ed) *Evolution of Geologic Structures in Micro to Macro-scale*. Chapman & Hall, London, 143-165.

MCCLAY, K. 1976. The rheology of plasticine. *Tectonophysics*, **33**, T7– T15.

MCCLAY, K., DOOLEY, T. & WHITEHOUSE O. 1999. Analogue modelling of thin and thick-skinned thrust systems, Thrust Tectonics Conference, Paper **18**, p 45. Geology Department, Royal Holloway University of London, Egham, England.

MCCLAY, K. R., WHITEHOUSE, P. S., DOOLEY, T. & RICHARDS, M. 2004. 3D evolution of fold and thrust belts formed by oblique convergence. *Marine and Petroleum*

Geology, **21**, 857-877.

McCLAY, K. R. & WHITEHOUSE, P. S. 2004. Analog Modeling of Doubly Vergent Thrust Wedges. *In:* McCLAY, K. (ed) *Thrust tectonics and hydrocarbon systems*. AAPG Memoir, **82**, 184–206.

MATTE, P. 1968. La structure de la virgation hercynienne de Galice (Espagne). *Géologie Alpine*, **44**.

MATTE, P. 2007. Variscan thrust nappes, detachments, and strike-slip faults in the French Massif Central: Interpretation of the lineations. *In:* HATCHER JR., R.D., CARLSON, M.P., McBRIDE, J.H. & MARTÍNEZ CATALÁN, J.R. (eds), *4-D Framework of Continental Crust.* Geological Society of America, Memoir, **200**, 391–402. Doi: 10.1130/2007.1200(20)

MOLLI, G. 2008. Northern Apennine-Corsica orogenic system: an updated overview. *In:* SIEGESMUND, S., FUGENSCHUH, B. & FROITZHEIM, N. (eds) *Tectonic Aspects of the Alpine-Dinaride-Carpathian System*. Geological Society, London, Special Publications, **298**, 413–442

MOLLI, G. & VASELLI, L. 2006. Structures, interference patterns and strain regime during mid-crustal deformation in the Alpi Apuane (Northern Apennine, Italy), *Geological Society of America,* Special Paper, 414, 79-93

MOLLI, G., GIORGETTI, G. & MECCHERI, M. 2002. Tectono-metamorphic evolution of

899 the Alpi Apuane Metamorphic Complex: new data and constraints for geodynamic
900 models. *Bollettino della Società Geologica Italiana,* volume speciale n.1, 789-800.
901
902 MOSAR J. 1999. Present-day and future tectonic underplating in the Western
903 SwissAlps: reconciliation of basement/wrench-faulting and décollement folding of the
904 Jura and Molasse Basin in the Alpine foreland. *Earth and Planetary Science Letters*,
905 **173/3***,* 143-155.
906
907 MUGNIER, J. L., BABY, P., COLLETTA, B., VINOUR, P., BALE, P. & LETURMY, P. 1997.
908 Thrust geometry controlled by erosion and sedimentation: A view from analogue
909 models. *Geology*, **25**, 427–430.
910
911 MULUGETA, G. 1988. Modelling the geometry of Coulomb thrust wedges. *Journal of*
912 *Structural Geology*, **10**, 847-859.
913
914 MULUGETA, G. & KOYI, H. 1992. Episodic accretion and strain partitioning in a model
915 sand wedge. *Tectonophysics*, **202**, 319-333.
916
917 NELSON, K. D., et al. 1996. Partially molten middle crust beneath southern Tibet:
918 Synthesis of project INDEPTH results, *Science*, **274**, 1684–1688,
919 doi:10.1126/science.274.5293.1684.
920
921 NICOLAS, A., BOUCHEZ, J. L., BLAISE, J. L. & POIRIER, J. P. 1977. Geological aspects
922 of deformation in continental shear-zones. *Tectonophysics*, **42**, 55-73, doi:
923 10.1016/0040-1951(77)90017-8.

NIEUWLAND, D. A., LEUTSCHER, J. H. & GAST, J. 2000. Wedge equilibrium in fold-and-thrust belts: prediction of out-of-sequence thrusting based on sandbox experiments and natural examples. *Netherlands Journal of Geosciences*, **79**, 81-91.

NOBLE, T. E. & DIXON, J. M. 2011. Structural evolution of fold-thrust structures in analog models deformed in a large geotechnical centrifuge. *Journal of Structural Geology*, **33**, 62–77

PÉREZ-ESTÀUN, A., MARTINEZ-CATALAN, J. R. & BASTIDA, F. 1991. Crustal thickening and deformation sequence in the footwall to the suture of the Variscan belt of NW Spain. *Tectonophysics*, **191**, 243–253

PERSSON, K. S. & SOKOUTIS, D. 2002. Analogue models of orogenic wedges controlled by erosion. *Tectonophysics*, **356**, 323-336.

PLATT, J. P., LEGGETT, J. K., YOUNG, J., RAZA, H. & ALAM, S. 1985. Large-scale sediment underplating in the Makran accretionary prism, southwest Pakistan: *Geology*, **13**, 507–511.

PRICE, R. A. 1981. The Cordilleran foreland thrust and fold belt in the southern Canadian Rocky Mountains. *In:* MCCLAY, K. & PRICE, N.J. (eds) *Thrust and nappe tectonics*. Geological Society, London, Special Publication, **9**, 427–448.

RAMBERG, H. 1981. *Gravity, deformation and the earth's crust*, 2nd edition,

Academic press, London. 452 pp.

RANALLI, G. 1995. *Rheology of the Earth*, 2nd edition, Chapman & Hall, London.

SCHELLART, W. P. 2000. Shear test results for cohesion and friction coefficients for different granular materials: scaling implications for their usage in analogue modelling. *Tectonophysics*, **324**, 1-16

SCHÖPFER, M. P. J. & ZULAUF, G., 2002. Strain dependent rheology and the memory of plasticine. *Tectonophysics*, **354**, 85–99.

SIMANCAS, J. F., AYARZA, P., AZOR, A., CARBONELL, R., MARTINEZ POYATOS, D., PÉREZ-ESTÀUN, A., GONZALEZ LODEIRO, F. A. A seismic geotraverse across the Iberian Variscides: orogenic shortening, collisional magmatism and orocline development. *Tectonics, in press,* doi : 10.1002/tect.20035

SMIT, J., BURG, J.-P., DOLATI, A. & SOKOUTIS, D. 2010. Effects of mass waste events on thrust wedges: Analogue experiments and application to the Makran accretionary wedge. *Tectonics*, **29**. TC3003, doi : 10.1029/2009TC002526

SOULA, J. C., DEBAT, P., BRUSSET, S., BESSIÈRE, G., CHRISTOPHOUL, F. & DÉRAMOND, J. 2001. Thrust-related, diapiric, and extensional doming in a frontal orogenic wedge: Example of the Montagne Noire, Southern French Hercynian Belt. *Journal of Structural Geology*, **23**, 1677–1699, doi:10.1016/ S0191-8141(01)00021-9.

974 STOCKMAL, G. S., BEAUMONT, C., NGUYEN, M. & LEE, B. 2007. Mechanics of thin-
975 skinned fold-and-thrust belts: Insights from numerical models. *In:* SEARS, J.W.,
976 HARMS, T. A. & EVENCHICK, C. A. (eds) *Whence the Mountains? Inquiries into the*
977 *evolution of orogenic systems: A volume in Honor of Raymond A. Price*. Geological
978 Society of America, Special Paper, **433**, 63–98.
979
980 STORTI, F. & MCCLAY, K. 1995. Influence of syntectonic sedimentation on thrust
981 wedges in analogue models. *Geology*, **23**, 999-1002.
982
983 SUTTON, J. & WATSON, J. V. 1986. Architecture of the continental lithosphere.
984 *Philosophical Transactions of the Royal Society, London*, **A317**, 5–12.
985
986 TIKOF, B. & PETERSON, K. 1998. Physical experiments of transpressional folding.
987 *Journal of Structural Geology*, **20**, 661-672
988
989 VAN DEN DRIESSCHE, J. & BRUN, J. P. 1992. Tectonic evolution of the Montagne
990 Noire (french Massif Central): a model of extensional gneiss dome: *Geodinamica*
991 *Acta*, **5**, 85–99.
992
993 WEBB, A. A. G., YIN, A., HARRISON, T. M., CELERIER, J. & BURGESS, W. P. 2007. The
994 leading edge of the Greater Himalayan Crystalline complex revealed in the NW
995 Indian Himalaya: Implications for the evolution of the Himalayan orogen, *Geology*,
996 **35**, 955–958, doi:10.1130/G23931A.1.
997
998 WEBB, A. A. G., SCHMITT A. K., HE, D. & WEIGAND E.L. 2011. Structural and

geochronological evidence for the leading edge of the Greater Himalayan Crystalline complex in the central Nepal Himalaya. *Earth and Planetary Science Letters*, **304**, 483–495.

ZULAUF, J. & ZULAUF, G. 2004. Rheology of plasticine used as rock analogue: the impact of temperature, composition and strain. *Journal of Structural Geology*, **26**, 725–737.

1007 **Figures and Captions**

1008

Experiment name	Total shortening *(cm)*	Protowedge		Lower plate		Decollement	Plastiline			Erosion		
		Length *(cm)*	Slope *(°)*	Total thickness *(cm)*	Termination	position* *(cm)*	Present	Thickness *(cm)*	Position* *(cm)*	Present	Start† *(cm)*	Slope
Exp 1	150	61	7	3.1	Straight	Top lower plate	No			No		
Exp 2	150	66	4	3.1	Straight	Top lower plate	No			No		
Exp 3	160	80	2	3.1	Gradual	Top lower plate	No			No		
Exp 4	180	74	0	3.1	Straight	1.1	No			No		
Exp 5	201	74	0	3.1	Straight	1.1	No			Yes	30	Variable
Exp 6	198	66	4	3.1	Straight	2.1	No			Yes	30	Variable
Exp 7	220	66	4	3.1	Straight	2.1	No			Yes	20	Fixed (5°)
Exp 8	160	80	2	3.3	Gradual	Top lower plate	Yes	0.3	1.7	No		
Exp 9	167	90	0	3.3	Gradual (-15cm)‡	Top lower plate	Yes	0.2	1	No		
Exp 10	163	90	0	3.3	Gradual (-15cm)‡	Top lower plate	Yes	0.1	1	No		
Exp 11	193	90	0	3.3	Gradual (-15cm)‡	Top lower plate	Yes	0.1	1	Yes	25	Fixed (5°)
Exp 12	175	80	2	3.3	Gradual	1.48	Yes	0.2	1.5	No		
Exp 13	200	90	0	3.5	Gradual (-15cm)‡	1	Yes	0.1	1.7	Yes	15	Fixed (3°)

Notes:

* Height from base plate

† Amount of initial shortening without erosion

‡ Lower plate ends before the backstop

1009

1010 **Table 1.** *Parameters used for the thirteen experiments.* (Models described in the text are in bold**)**

1011

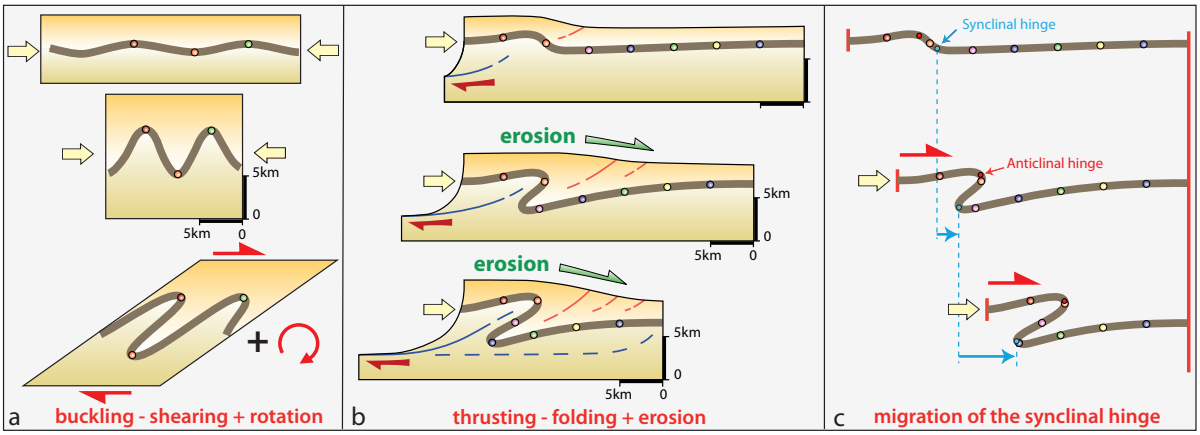

Fig. 1.

Fig. 1. Cartoon showing two folding mechanisms to generate large-scale overturned folds in fold and thrust belts. The first mechanism involve an important burial whereas the second one allows the development of large folds with slight burial. (a) Buckling and folding during compressional shortening followed by shearing and tilting of fold limbs; (b) Fold amplification by thrusting and subsequent shearing, unrolling and migration of the synclinal hinge in the frame of a fold and thrust wedge; (c) Simplified kinematic sketch of the same process. Coloured circles are passive markers regularly spaced in the folded layer.

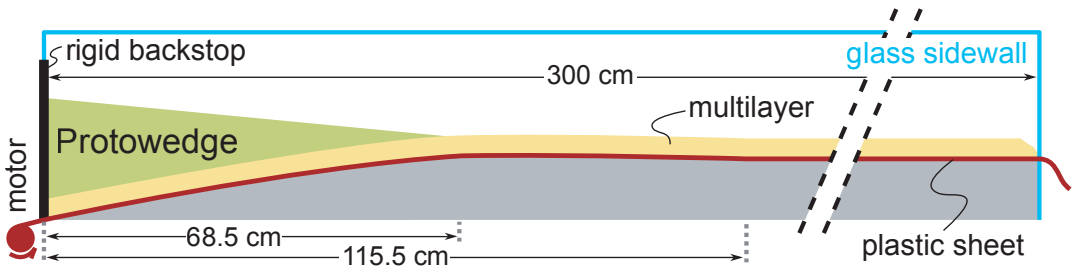

Fig. 2

Fig. 2. Experimental set-up. The width of the device is 10 cm.

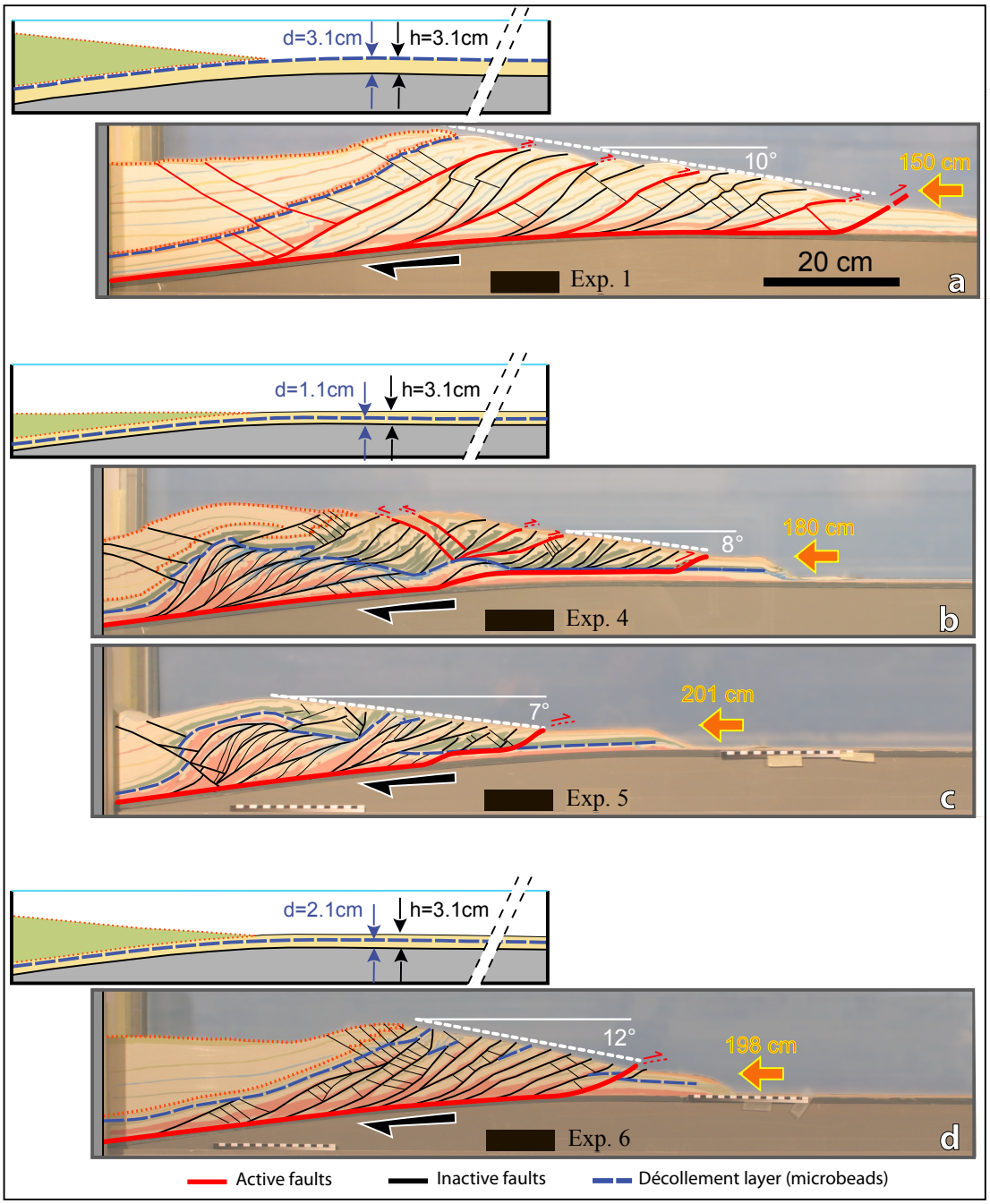

Fig. 3

Fig. 3. Initial configuration and final result of models involving a microbeads layer located at different heights ("d" on sketch). (a) Classical high friction thrust wedge. The thrust front propagates in a piggy-back style, but some faults remain active after the nucleation of new faults at the front. (b) Strain partitioning: duplexing at the base of the wedge and frontal accretion at the toe. Note the cyclical behavior of underplating. (c) Impact of surface erosion on the wedge dynamics, location of

underplating and exhumation of underplated units. (d) Underplating is inhibited when décollement is too shallow. Shortening in cm on digital screen.

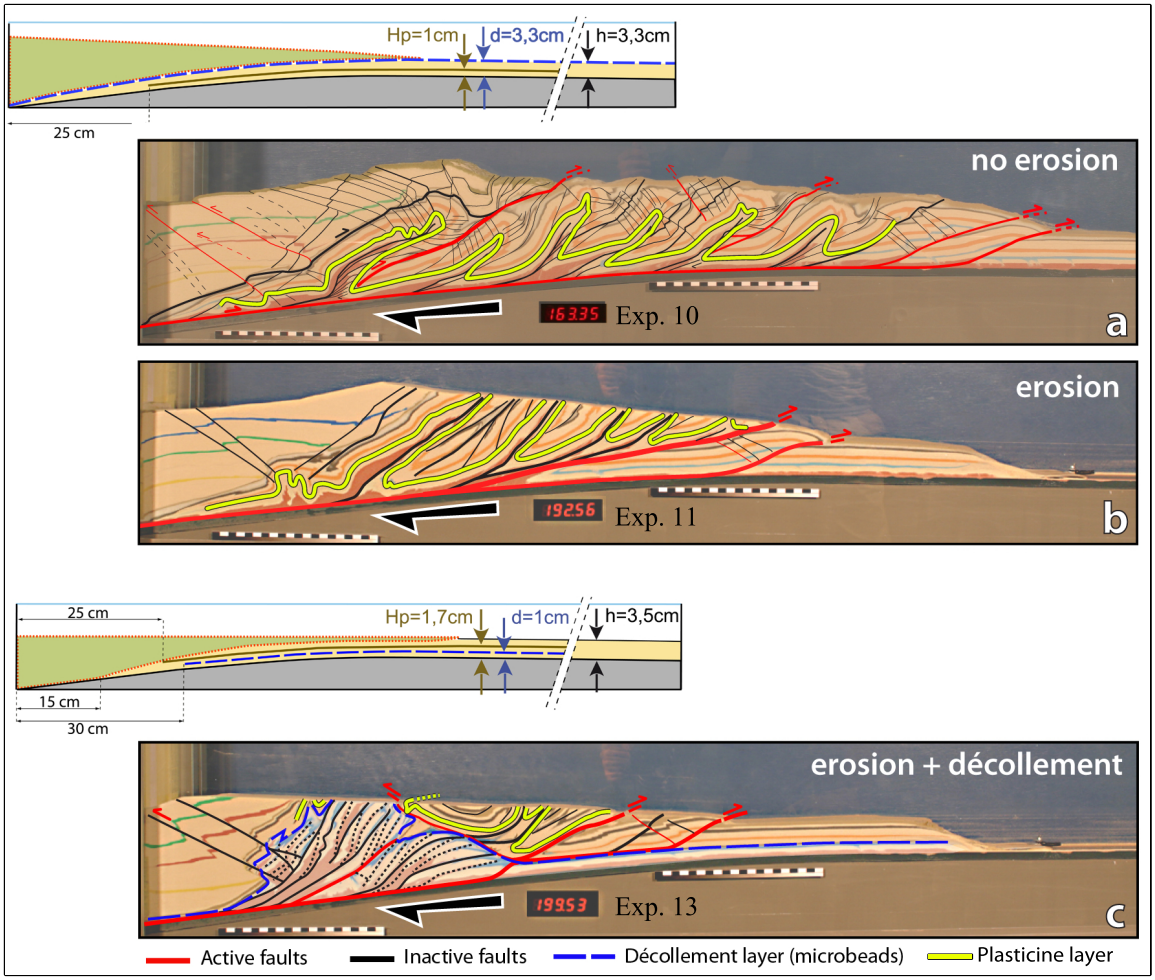

Fig. 4

Fig. 4. Initial setting and final stage of model involving a thin layer of plasticine (Hp: Height of the plasticine layer on sketch). (a) Case no erosion. Folds are overturned with an angle between 30° and 50°; (b) Same experiment with erosion; (c) Brittle/plastic model with décollement layer and erosion. Shortening in cm on digital screen.

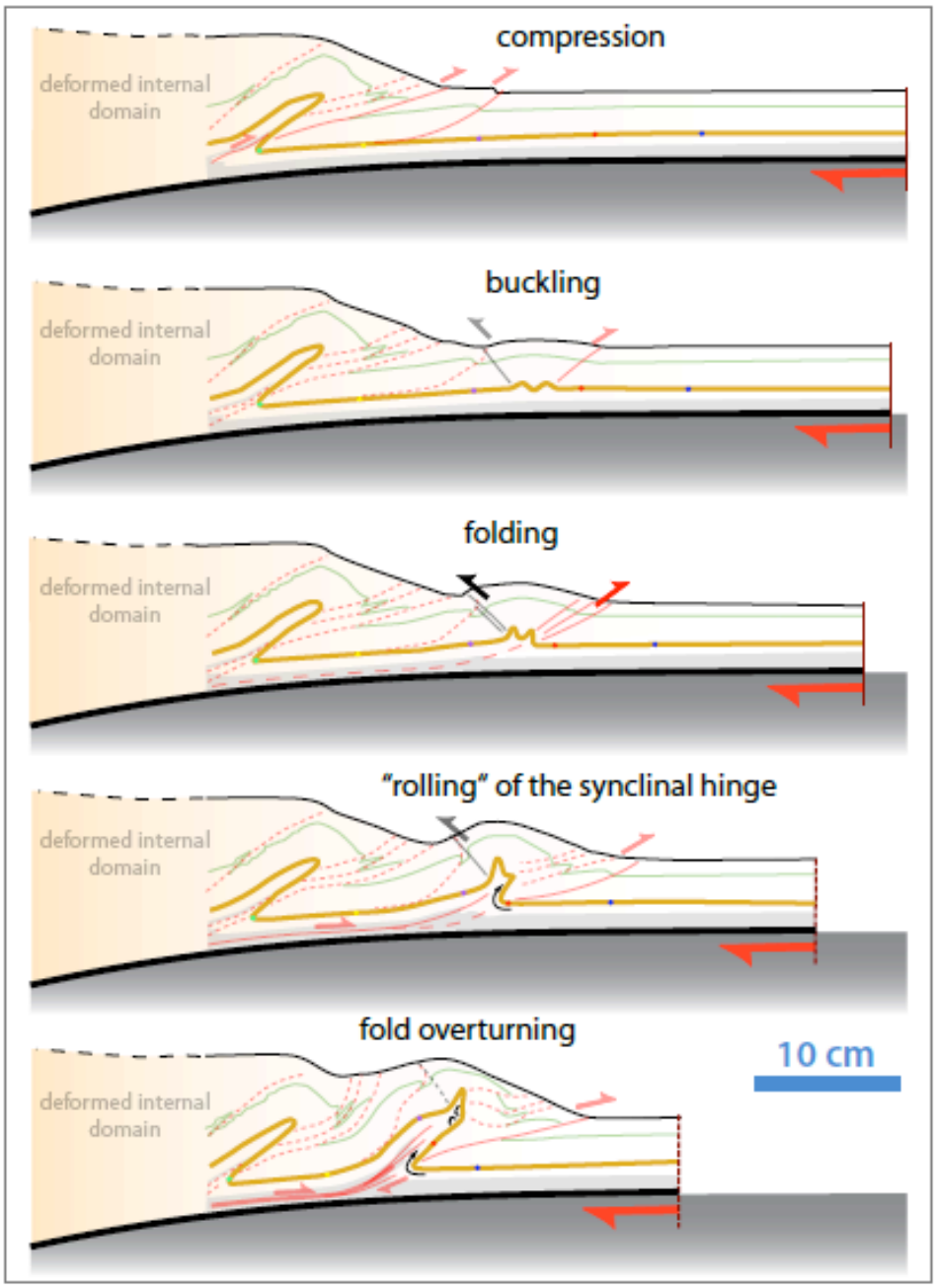

Fig. 5

Fig. 5. Kinematic model of folding. The thick line with circles represents the plasticine with displacement indicators.

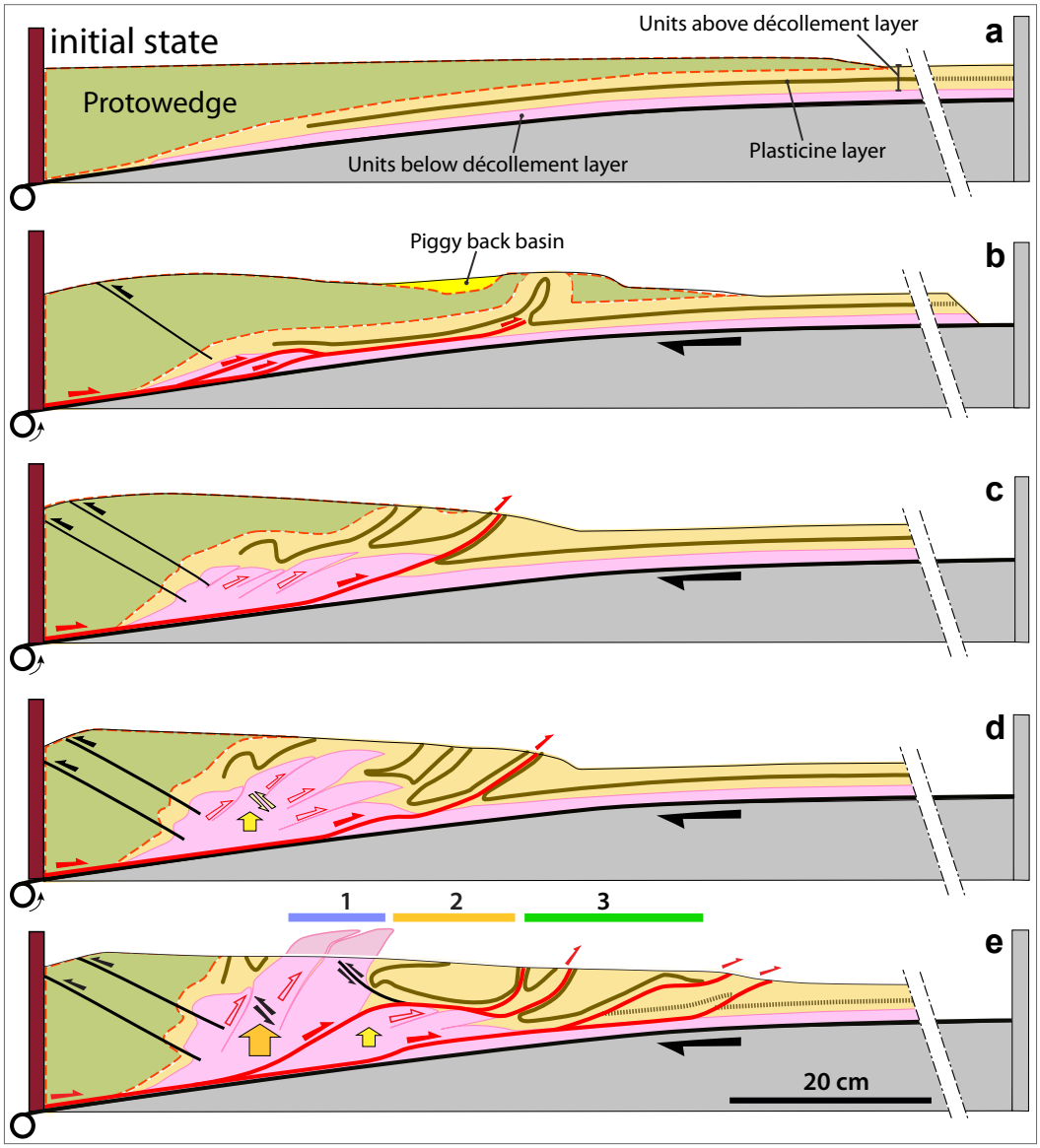

Fig. 6

Fig. 6. Evolution of complex model involving brittle/plastic multilayer, erosion and décollement layer. Upper units situated above décollement layer are composed of sand and plasticine; deep units below décollement layer are composed of sand. At the final stage (e), three domains are juxtaposed: (1) exhumation of deep rocks, (2) the domain of recumbent folds and (3) the overturned folds.

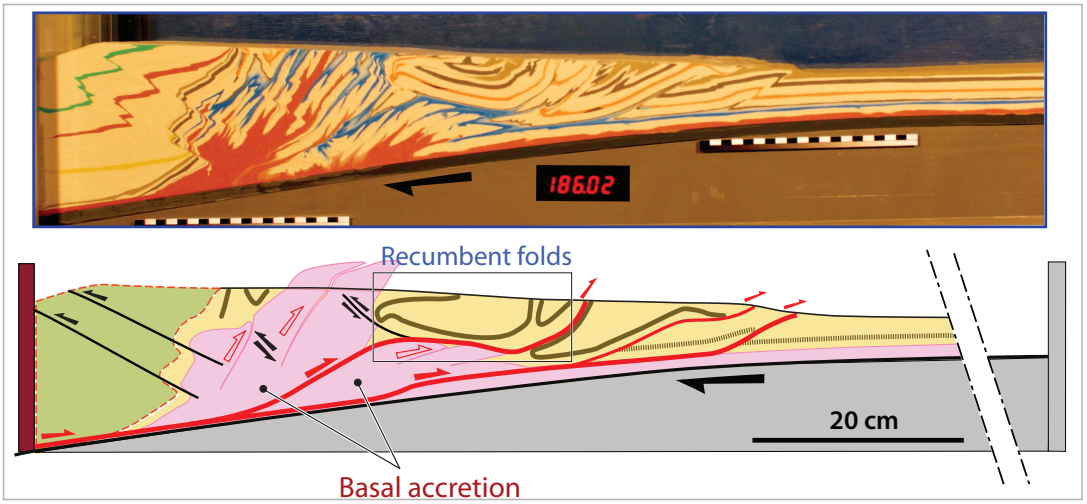

Fig.7

Fig. 7. Relationships between cyclical duplexing and kinematics of folding in a brittle/plastic model with erosion and décollement level.

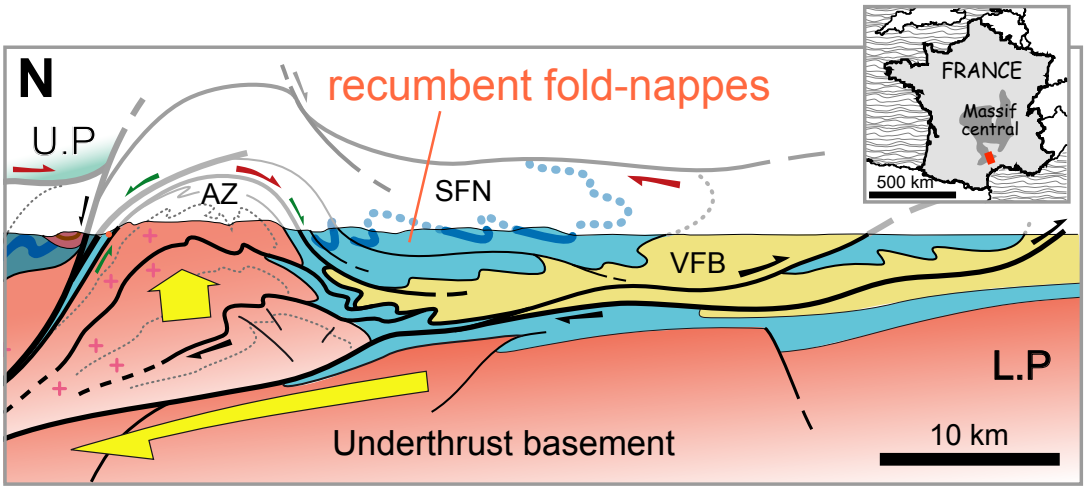

Fig. 8

Fig. 8. Cross-section of the Montagne Noire, southern part of French Massif Central (modified from Malavieille 2010). U.P.: Upper Plate, L.P.: Lower Plate. AZ: Axial Zone, SFN: Southern Fold Nappes, VFB: Visean Foreland Basin.

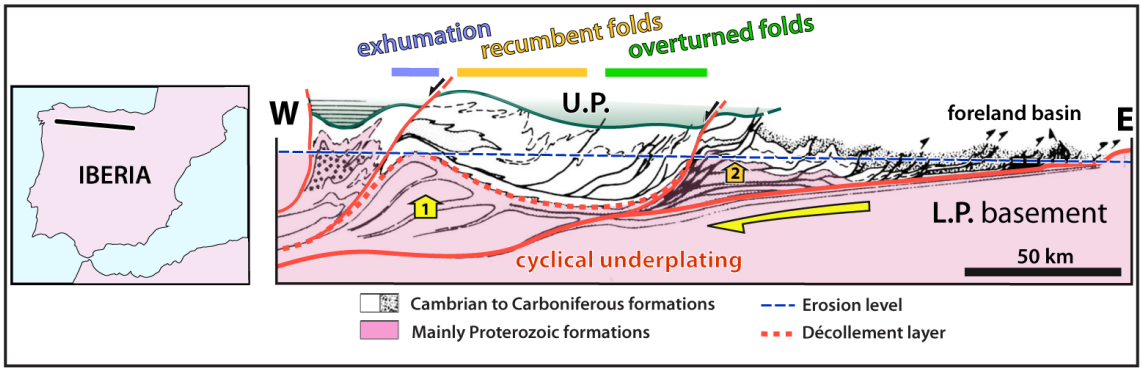

Fig.9

Fig. 9. Cross-section of Variscan Belt in Galicia, Spain (modified from Pérez-Estàun *et al*. 1991). U.P.: Upper Plate; L.P.: Lower Plate.

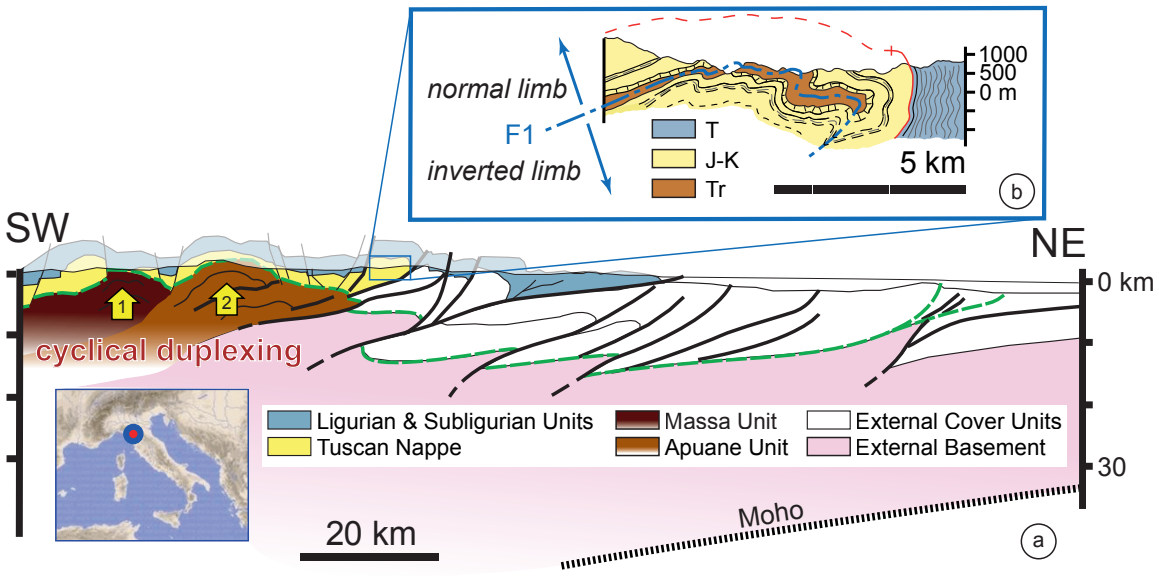

Fig. 10

Fig. 10. (a) Cross section of the Northern Apennines, Italy (modified from Molli 2008). (b) Cross-section of the Val di Lima fold structure (modified from Baldacci *et al*. 1992). T: Tertiary; J-K: Jurassic-Cretaceous; Tr: Triassic.